




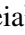
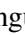

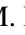




On the Numerical Solution of the Inverse Elastography Problem for Time-harmonic Excitation

Pedro Serranho^{1,2}^a, Sílvia Barbeiro³^b, Rafael Henriques³^c, Ana Batista²^d, Mário J. Santos⁴^e,
Carlos Correia²^f, José P. Domingues⁵^g, Custódio Loureiro⁵^h, João M. R. Cardoso⁵ⁱ,
Rui Bernardes^{2,6}^j and Miguel Morgado^{2,5}^k

¹Department of Science and Technology, Universidade Aberta, Rua da Escola Politécnica, 147, 1269-001, Lisbon, Portugal

²Coimbra Institute for Biomedical Image and Translational Research, Faculty of Medicine, University of Coimbra, Edifício do ICNAS, Polo 3 Azinhaga de Santa Comba 3000-548, Coimbra, Portugal

³University of Coimbra, CMUC - Center of Mathematics, Department of Mathematics, Apartado 3008, EC Santa Cruz, 3001-501, Coimbra, Portugal

⁴University of Coimbra, Department of Electrical and Computer Engineering, Faculty of Science and Technology, Pólo II, 3030-290, Coimbra, Portugal

⁵Department of Physics, University of Coimbra, Rua Larga, 3004-516, Coimbra, Portugal

⁶University of Coimbra, CACC-Clinical Academic Center of Coimbra, Faculty of Medicine (FMUC), Coimbra, Portugal

Keywords: Numerical Methods, Method of Fundamental Solutions, Elastography, Optical Coherence Elastography.

Abstract: In this paper we address the numerical solution of the inverse elastography problem, from the knowledge of the excitation field on the boundary and the displacement field in a grid of points within the domain. We suggest using a representation of the solution by the method of fundamental solutions and using a Newton-type method to iteratively approximate the Lamé coefficients of the medium from elastography displacement measurements. We consider a toy model to illustrate the performance of the method.


1 INTRODUCTION


Elastography is an imaging modality where the elastic displacement induced by a given excitation on the imaged tissue is measured to recover the material's elastic properties.


We are especially interested in considering optical coherence elastography (OCE), which means that one used optical coherence tomography to measure the


phase difference related to the elastic movement and the consequent elastic displacement in depth of the tissue (see, for instance (Claus et al., 2017; Kennedy et al., 2011; Qu et al., 2018; Zhu et al., 2017)). Therefore, one is interested in recovering the elastic properties of the tissue material given the measurement of the depth displacement in a grid of inner points within the tissue and the time-harmonic excitation.


This paper will consider time-harmonic excitation for the Lamé equation, which allows the elastic field to be represented by the method of fundamental solutions (MFS). In this case, we propose a Newton's method approach based on the differentiation of the operator that maps the Lamé coefficients to the solution of the problem. At each iteration the proposed method requires few computational effort to update the Lamé coefficients, since it resumes to solve a 2-by-2 linear system at each iteration. However, to establish this linear system a forward problem must be solved at each iteration, which supports the choice of a MFS approach due to its easy implementation. We


^a <https://orcid.org/0000-0003-2176-3923>


^b <https://orcid.org/0000-0002-2651-5083>


^c <https://orcid.org/0000-0003-4173-8469>


^d <https://orcid.org/0000-0002-5672-8266>


^e <https://orcid.org/0000-0002-0188-7761>


^f <https://orcid.org/0000-0002-2947-1880>

^g <https://orcid.org/0000-0002-0562-8994>

^h <https://orcid.org/0000-0001-7856-2124>

ⁱ <https://orcid.org/0000-0002-8832-8208>

^j <https://orcid.org/0000-0002-6677-2754>

^k <https://orcid.org/0000-0001-9455-1206>

also discuss the main advantages and possible disadvantages of this approach.

2 PROBLEM FORMULATION

For time-harmonic waves, the Lamé equation governs the elastic displacement field u in a domain D (Doyley, 2012; Park and Maniatty, 2006) by

$$\mu \Delta u + (\lambda + \mu) \operatorname{grad} \operatorname{div} u + \omega^2 \rho u = 0 \text{ in } D, \quad (1)$$

where ρ is the density, ω is the frequency, and the Lamé constants are given by

$$\mu = \frac{E}{2(1+\nu)}, \quad \lambda = \frac{\nu E}{(1+\nu)(1-2\nu)},$$

where ν is the Poisson's ratio and E is the Young's Modulus. Usually in this setting the boundary conditions are defined by the pressure p , namely by relating it with the elastic field u at some part Γ of the boundary ∂D by one or both of the following transmission conditions (Ito et al., 2008; Ito and Toivanen, 2007)

$$\frac{1}{\rho} \frac{\partial p_{n-1}}{\partial \nu} = \omega^2 u \cdot \nu \text{ on } \Gamma, \quad (2)$$

$$p_{n-1} \nu_{n-1} = \sigma(u) \nu_n \text{ on } \Gamma, \quad (3)$$

where the stress tensor is given by

$$\sigma(u) = \mu(\nabla u + (\nabla u)^T) + \lambda \operatorname{div} u I.$$

In the remaining boundary, one can assume either

$$u = 0 \text{ on } \partial D \setminus \Gamma \quad (4)$$

or

$$\sigma(u) \nu = 0 \text{ on } \partial D \setminus \Gamma. \quad (5)$$

The setting of the problem is illustrated in figure 1.

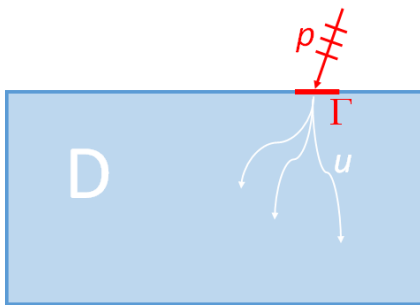


Figure 1: Problem and Domain setting.

The direct problem consists in determining the elastic field u within the domain D , given the pressure p on Γ , the material's density ρ , the frequency ω and Lamé coefficients μ and λ . This can be done using a forward solver as for instance the MFS, which we will detail in the following section.

The inverse problem consists in determining the Lamé coefficients μ and λ from the knowledge of elastic field u in a discrete grid of points in domain D , the pressure p on Γ , the material's density ρ and the frequency ω . The following section will address the proposed numerical approach based on Newton's method to solve the inverse problem.

3 NUMERICAL METHOD

Having in mind that the fundamental solution of equation (1) in \mathbb{R}^2 is given by (cf. (Alves et al., 2017))

$$\begin{aligned} \Phi(x) = & \frac{i}{4\rho\omega^2} \left(\kappa_s^2 H_0^{(1)}(\kappa_s|x|)I \right. \\ & \left. + \operatorname{grad} \operatorname{grad}(H_0^{(1)}(\kappa_s|x|) - H_0^{(1)}(\kappa_p|x|)) \right) \end{aligned} \quad (6)$$

where

$$\kappa_p^2 = \frac{\omega^2 \rho}{\lambda + 2\mu}, \quad \kappa_s^2 = \frac{\omega^2 \rho}{\mu}, \quad (7)$$

$H_n^{(1)}$ is the Hankel function of first kind and order n , I is the identity operator in \mathbb{R}^2 and one has

$$\begin{aligned} \operatorname{grad} \operatorname{grad}(H_0^{(1)}(\kappa|x|)) = & \kappa^2 \frac{x \cdot x^T}{|x|^2} H_2^{(1)}(\kappa|x|) \\ & - \frac{\kappa}{|x|} H_1^{(1)}(\kappa|x|)I, \end{aligned}$$

the method of fundamental solutions is based on the representation of the solution as

$$u(x; \kappa_s, \kappa_p) = \sum_{k=1}^{N_s} \Phi(x - s_k) \alpha_k \quad (8)$$

for some source points $s_k \notin \bar{D}$, $k = 1, 2, \dots, N_s$, and coefficients $\alpha_k \in \mathbb{C}^2$. From the definition of fundamental solution, it can be shown that this representation fulfils equation (1). Moreover, it can be shown that solutions of this form are dense for analytic solutions of the problem (Alves et al., 2017).

Therefore, the method of fundamental solutions is a good choice for forward solver (cf. (Barbeiro and Serrano, 2020)), since one needs only to find the coefficients $\alpha_k \in \mathbb{C}^2$ such that the boundary conditions (2)-(3) and (4) or (5) are satisfied.

Given the elastography data, that is, the measurement points $x_j \in D$, $j = 1, 2, \dots, N_m$ and the respective displacement measures $u_j = u(x_j)$, we now define the operators

$$G_j : (\kappa_s, \kappa_p) \mapsto u(x_j; \kappa_s, \kappa_p) - u_j, \quad j = 1, 2, \dots, N_m.$$

In this way, one wants to find κ_s, κ_p such that

$$G_j(\kappa_s, \kappa_p) = 0, \quad \forall j = 1, 2, \dots, N_m.$$

To achieve this, we propose a Newton's method approach. At iteration n , given the current approximations $(\kappa_s^{(n)}, \kappa_p^{(n)})$ one solves the system of N_m equations

$$\begin{aligned} \frac{\partial G_j}{\partial \kappa_s}(\kappa_s^{(n)}, \kappa_p^{(n)}) h_s + \frac{\partial G_j}{\partial \kappa_p}(\kappa_s^{(n)}, \kappa_p^{(n)}) h_p \\ = -G_j(\kappa_s^{(n)}, \kappa_p^{(n)}) \end{aligned}$$

with respect to (h_s, h_p) in a least square sense, having the new update

$$\kappa_s^{(n+1)} = \kappa_s^{(n)} + h_s, \quad \kappa_p^{(n+1)} = \kappa_p^{(n)} + h_p.$$

The method is now iterated until some stopping criteria is achieved. It is also worth noting that in this case one has

$$\frac{\partial G_j}{\partial \kappa_s}(\kappa_s, \kappa_p) = \frac{\partial u}{\partial \kappa_s}(x_j; \kappa_s, \kappa_p) \quad (9)$$

$$\frac{\partial G_j}{\partial \kappa_p}(\kappa_s, \kappa_p) = \frac{\partial u}{\partial \kappa_p}(x_j; \kappa_s, \kappa_p) \quad (10)$$

However, in particular for OCE one only gathers the displacement in depth, so in this case the operator G_j should be modified to

$$G_{2,j} : (\kappa_s, \kappa_p) \mapsto u_2(x_j; \kappa_s, \kappa_p) - u_{2,j}$$

that is, one has only access to the second component of the displacement vector.

We also note that the problem of recovering (κ_s, κ_p) is equivalent to recovering (μ, λ) , since one pair uniquely defines the other by (7).

4 PRELIMINARY NUMERICAL RESULTS

The numerical results we present here are ongoing work, so you will only consider a simple toy model. Moreover, tuning of the parameters has not yet been considered, so the results might improve.

We consider D to be a unit circle. Instead of the boundary conditions (2)-(5), we considered the Dirichlet boundary condition in all of $x \in \partial D$ given by

$$u(x) = 0.25 \exp(ikd \cdot x) \exp(-|x - (0, 1)|^2 / 0.25) \mathbf{v} \quad (11)$$

with $d = (-1, -5) / \sqrt{26}$, $\kappa = 1$ and \mathbf{v} is the outward normal unit vector to the boundary. Also, we considered $\omega = \rho = 1$. For the forward problem, we considered 800 collocation points equally spaced over the unit circumference and 400 source points over the circumference of radius $r=1.2$, for the

MFS representation (8). We considered Tikhonov regularization to solve the overdetermined linear system to determine α_k in (8) by imposing (11) on the collocation points. This procedure obtained the displacement field u_j in a grid of points x_j as illustrated in figure 2, for example 1.

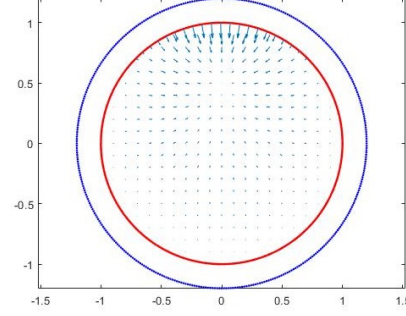


Figure 2: Displacement field data u_j in the measurement points x_j and displacement given by boundary condition for example 1 ($\kappa_s = 0.5, \kappa_p = 2$), with 400 source points (blue) and 800 collocation points (red).

To avoid an inverse crime (Colton and Kress, 2013), for the inverse problem we considered 200 collocation points equally spaced over the unit circumference and 100 source points equally spaced over the circumference of radius $r=1.1$, for the forward MFS solver considering the current approximation for the parameters $(\kappa_s^{(n)}, \kappa_p^{(n)})$, with the same regularization parameter.

We considered the error norm

$$\|G_2^{(n)}\|_{\ell^2} = \sqrt{\sum_{j=1}^{N_m} G_{2,j}(\kappa_s^{(n)}, \kappa_p^{(n)})^2}$$

and stop the algorithm whenever this error increases from one iteration to the following. We also define the error in the approximation

$$e_s^{(n)} = |\kappa_s^{(n)} - \kappa_s|, \quad e_p^{(n)} = |\kappa_p^{(n)} - \kappa_p|.$$

We started by considering $\kappa_s = 0.5$ and $\kappa_p = 2$ in example 1. The results are shown in Table 1 for exact data and in Table 2 for multiplicative 1% noise in the data. We can see that for exact data the approximation has high precision and is not very affected with noise. As for example 2, we considered $\kappa_s = 1.2$ and $\kappa_p = .5$, with results in Table 3 for exact data and in Table 4 for multiplicative 1% noise in the data. In this case the method seems to stop very early for exact data. This is clear once for noisy data, the method performs at a very similar level. Future work should consider optimization of the regularization coefficient based on error and/or number of points.

Table 1: Results for exact data for example 1: $\kappa_s = 0.5, \kappa_p = 2$.

n	$\kappa_s^{(n)}$	$\kappa_p^{(n)}$	$e_s^{(n)}$	$e_p^{(n)}$	$\ G_2^{(n)}\ _{\ell^2}$
0	1	1	0.5	-1	0.036015
1	0.85337	1.2119	0.35337	-0.78813	0.022349
5	0.46939	1.4692	-0.030611	-0.53076	0.0041958
10	0.44448	1.588	-0.055522	-0.41196	0.0028442
50	0.49623	1.9429	-0.0037699	-0.057122	0.00047919
100	0.49975	1.9951	-0.00025248	-0.0049319	$4.2702e^{-5}$
200	0.50000	2.0000	$-1.3591e^{-6}$	$-3.3625e^{-5}$	$3.1419e^{-7}$
249	0.50000	2.0000	$3.3361e^{-7}$	$3.5057e^{-7}$	$1.0881e^{-7}$
250	0.50000	2.0000	$3.4172e^{-7}$	$5.1348e^{-7}$	$1.0882e^{-7}$

Table 2: Results for 1% noisy data for example 1: $\kappa_s = 0.5, \kappa_p = 2$.

n	$\kappa_s^{(n)}$	$\kappa_p^{(n)}$	$e_s^{(n)}$	$e_p^{(n)}$	$\ G_2^{(n)}\ _{\ell^2}$
0	1	1	0.5	-1	0.036014
1	0.85332	1.2117	0.35332	-0.7883	0.022352
5	0.46871	1.4684	-0.031286	-0.53156	0.0041952
10	0.44344	1.5865	-0.056559	-0.4135	0.0028518
50	0.49489	1.9389	-0.0051093	-0.061051	0.00053961
100	0.49845	1.9908	-0.0015487	-0.0092421	0.00020766
200	0.49871	1.9956	-0.0012923	-0.0043913	0.00019709
424	0.49871	1.9956	-0.0012904	-0.0043545	0.00019704

Table 3: Results for exact data for example 2: $\kappa_s = 1.2, \kappa_p = 0.5$.

n	$\kappa_s^{(n)}$	$\kappa_p^{(n)}$	$e_s^{(n)}$	$e_p^{(n)}$	$\ G_2^{(n)}\ _{\ell^2}$
0	0.8	0.8	-0.4	0.3	0.02538
1	0.95237	0.70177	-0.24763	0.20177	0.01406
5	1.0882	0.60583	-0.11183	0.10583	0.0057529
10	1.14	0.55603	-0.059973	0.056034	0.0028045
20	1.1719	0.50782	-0.028133	0.0078185	0.00070746
30	1.1779	0.48971	-0.022086	-0.010286	0.00011391
34	1.178	0.48604	-0.021955	-0.013962	$8.4068e^{-5}$

Table 4: Results for 1% noisy data for example 2: $\kappa_s = 1.2, \kappa_p = 0.5$.

n	$\kappa_s^{(n)}$	$\kappa_p^{(n)}$	$e_s^{(n)}$	$e_p^{(n)}$	$\ G_2^{(n)}\ _{\ell^2}$
0	0.8	0.8	-0.4	0.3	0.025379
1	0.95227	0.70148	-0.24773	0.20148	0.014052
5	1.0877	0.60483	-0.11231	0.10483	0.0057361
10	1.1391	0.55427	-0.060947	0.054272	0.0027864
20	1.1697	0.50482	-0.030252	0.0048246	0.00074093
30	1.1745	0.48572	-0.0255	-0.014282	0.00035822
32	1.1744	0.48353	-0.025616	-0.016473	0.00035996

5 FINAL REMARKS AND PERSPECTIVES

The application of Newton’s method for inverse problems is common (Kress, 2003) and convergence as

been proven for some settings of ill-posed inverse problems (Hohage, 1998; Potthast, 2001). Also, the idea of using a reconstruction of field using the current approximation of the unknowns and a subsequent iteration based on the derivative of the operator that

maps the unknowns to the field has been successfully used in shape reconstruction of unknown obstacles in acoustics (Kress and Serranho, 2005; Kress and Serranho, 2007; Serranho, 2006; Serranho, 2007), so the use of a similar idea in elastodynamics seems promising.

The use of MFS for the direct elastography problem was also successful (Barbeiro and Serranho, 2020), supporting our choice for the ansatz of the elastic field. However, the solution of the inverse problem is, as usual, more complex. Newton's method worked well on our toy model, but more experiments need to be made. The method seems very sensitive to the choice of the initial guess $(\kappa_s^{(0)}, \kappa_p^{(0)})$ as usually in the application of Newton's method for ill-posed problems. In addition, the radius of the circumference for the source points, the choice of regularization parameters and the number of collocation and source points also affect the results. Moreover, we only considered low frequencies. High frequencies increase the ill-posedness and require more source points, turning the numerical solution more complex. These aspects should be addressed in future research.

Finally, domains with corners as in figure 1 or non-smooth initial conditions will require the enrichment of the basis functions of fundamental solutions with particular solutions that can cope with those singularities and discontinuities, in the spirit of (Alves et al., 2018). This will also be addressed in further research, since it allows the method to be applied in a setting as in figure 1 that is closer to elastography applications.

ACKNOWLEDGEMENTS

The authors would like to acknowledge their work is partially supported by FEDER Funds through the Operational Program for Competitiveness Factors - COMPETE and by Portuguese National Funds through FCT - Foundation for Science and Technology under the PTDC/EMD-EMD/32162/2017 project.

REFERENCES

- Alves, C. J., Martins, N. F., and Valtchev, S. S. (2017). Extending the method of fundamental solutions to non-homogeneous elastic wave problems. *Applied Numerical Mathematics*, 115:299 – 313.
- Alves, C. J., Martins, N. F., and Valtchev, S. S. (2018). Trefftz methods with cracklets and their relation to bem and mfs. *Engineering Analysis with Boundary Elements*, 95:93–104.
- Barbeiro, S. and Serranho, P. (2020). *The Method of Fundamental Solutions for the Direct Elastography Problem in the Human Retina*, pages 87–101. Springer International Publishing, Cham.
- Claus, D., Mlikota, M., Geibel, J., Reichenbach, T., Pedrini, G., Mischinger, J., Schmauder, S., and Osten, W. (2017). Large-field-of-view optical elastography using digital image correlation for biological soft tissue investigation. *Journal of Medical Imaging*, 4(1):1 – 14.
- Colton, D. and Kress, R. (2013). *Inverse Acoustic and Electromagnetic Scattering Theory*. Springer, 3rd edition.
- Doyley, M. M. (2012). Model-based elastography: a survey of approaches to the inverse elasticity problem. *Physics in Medicine and Biology*, 57(3):R35–R73.
- Hohage, T. (1998). Convergence rates of a regularized newton method in sound-hard inverse scattering. *SIAM J. Numer. Anal.*, 36:125–142.
- Ito, K., Qiao, Z., and Toivanen, J. (2008). A domain decomposition solver for acoustic scattering by elastic objects in layered media. *J. Comput. Phys.*, 227(19):8685–8698.
- Ito, K. and Toivanen, J. (2007). A fast iterative solver for scattering by elastic objects in layered media. *Applied Numerical Mathematics*, 57(5):811 – 820. Special Issue for the International Conference on Scientific Computing.
- Kennedy, B. F., Liang, X., Adie, S. G., Gerstmann, D. K., Quirk, B. C., Boppart, S. A., and Sampson, D. D. (2011). In vivo three-dimensional optical coherence elastography. *Opt. Express*, 19(7):6623–6634.
- Kress, R. (2003). Newton's method for inverse obstacle scattering meets the method of least squares. *Inverse Problems*, 19:91–104.
- Kress, R. and Serranho, P. (2005). A hybrid method for two-dimensional crack reconstruction. *Inverse Problems*, 21:773–784.
- Kress, R. and Serranho, P. (2007). A hybrid method for sound-hard obstacle reconstruction. *Journal of Computational and Applied Mathematics*, 204:418–427.
- Park, E. and Maniatty, A. M. (2006). Shear modulus reconstruction in dynamic elastography: time harmonic case. *Physics in Medicine and Biology*, 51(15):3697–3721.
- Potthast, R. (2001). On the convergence of a new newton-type method in inverse scattering. *Inverse Problems*, 17:1419–1434.
- Qu, Y., He, Y., Zhang, Y., Ma, T., Zhu, J., Miao, Y., Dai, C., Humayun, M., Zhou, Q., and Chen, Z. (2018). Quantified elasticity mapping of retinal layers using synchronized acoustic radiation force optical coherence elastography. *Biomed. Opt. Express*, 9(9):4054–4063.
- Serranho, P. (2006). A hybrid method for inverse scattering for shape and impedance. *Inverse Problems*, 22:663–680.

- Serranho, P. (2007). A hybrid method for inverse scattering for sound-soft obstacles in 3D. *Inverse Problems and Imaging*, 4:691–712.
- Zhu, J., Miao, Y., Qi, L., Qu, Y., He, Y., Yang, Q., and Chen, Z. (2017). Longitudinal shear wave imaging for elasticity mapping using optical coherence elastography. *Applied Physics Letters*, 110(20):201101.

